RNA Interference Screen to Identify Pathways That Enhance or Reduce Nonviral Gene Transfer During Lipofection

Gregory A Barker[1] and Scott L Diamond[1]

[1]Penn Center for Molecular Discovery, Institute for Medicine and Engineering, Department of Chemical and Biomolecular Engineering, University of Pennsylvania, Philadelphia, Pennsylvania, USA

Some barriers to DNA lipofection are well characterized; however, there is as yet no method of finding unknown pathways that impact the process. A druggable genome small-interfering RNA (siRNA) screen against 5,520 genes was tested for its effect on lipofection of human aortic endothelial cells (HAECs). We found 130 gene targets which, when silenced by pooled siRNAs (three siRNAs per gene), resulted in enhanced luminescence after lipofection (86 gene targets showed reduced expression). In confirmation tests with single siRNAs, 18 of the 130 hits showed enhanced lipofection with two or more individual siRNAs in the absence of cytotoxicity. Of these confirmed gene targets, we identified five leading candidates, two of which are isoforms of the regulatory subunit of protein phosphatase 2A (PP2A). The best candidate siRNA targeted the *PPP2R2C* gene and produced a 65% increase in luminescence from lipofection, with a quantitative PCR–validated knockdown of ~76%. Flow cytometric analysis confirmed that the silencing of the *PPP2R2C* gene resulted in an improvement of 10% in transfection efficiency, thereby demonstrating an increase in the number of transfected cells. These results show that an RNA interference (RNAi) high-throughput screen (HTS) can be applied to nonviral gene transfer. We have also demonstrated that siRNAs can be co-delivered with lipofected DNA to increase the transfection efficiency *in vitro*.

Received 23 May 2008; accepted 18 June 2008; published online 15 July 2008. doi:10.1038/mt.2008.147

INTRODUCTION

The basic mechanisms required for effective nonviral gene transfer are well established. During lipofection and polyfection, plasmid DNA (pDNA) must undergo endocytosis, escape the endo-lysosomal pathway, avoid nuclease degradation, and successfully traffic across cytoplasmic barriers before finally becoming localized in the nucleus.[1–3] Although these intracellular and extracellular barriers have been well studied, the transfection efficiency of nonviral vectors is low, especially in comparison with viral vectors, and more so in nondividing cells.

In order to understand mechanistic pathways in biology, RNA interference (RNAi)-mediated gene silencing has been used in combination with high-throughput screening (HTS) techniques. For example, RNAi screens have been used to study cell-cycle regulation and mitotic spindle assembly,[4,5] and the breadth of knowledge in respect of oncological pathways continues to expand with the application of RNAi HTS.[6,7] Recent work has involved the application of RNAi HTS to the study of host factors that play an important role in human immunodeficiency virus-1 infection.[8]

Each pairing of gene transfer reagent and host cell may have unique proteins that are important or inhibitory to gene transfer. An RNAi HTS is one approach to scan gene pathways in the context of specific pairings of lipofection protocol and cell host. In order to enable a better understanding of nonviral gene transfer, we developed a small-interfering RNA (siRNA) screen targeting 5,520 genes with three pooled siRNAs per gene in adult human aortic endothelial cells (HAECs). After siRNA delivery, the cells were lipofected with a Renilla luciferase plasmid. The separate luminescent signals from lipofection and cell viability were used for quantifying changes in lipofection efficiency. The siRNA pools identified as hits in the primary screen were rescreened as individual siRNAs and confirmed in larger-scale experiments. Interestingly, several of the top gene candidates were found to be cell-cycle-regulatory or involved in human immunodeficiency virus-1 infection.[9]

RESULTS

Assay development

In order to study the effect of siRNA-mediated knockdown on nonviral gene transfer, we developed an RNAi HTS assay. The siRNA library targets 5,520 druggable gene targets, with three siRNAs per gene. The three siRNAs for each gene were pooled such that the total siRNA concentration at the time of screening was 30 nmol/l. For screening the library, siRNAs were reverse transfected into HAECs, followed a day later by lipofection of a Renilla luciferase pDNA. One day later, luminescent signals from the Renilla pDNA lipofection and from a separate assay for cell viability were collected for each well; normalized transfection was calculated by dividing the luminescence from lipofection by the luminescence from viability.

Correspondence: *Scott L. Diamond, Penn Center for Molecular Discovery, Institute for Medicine and Engineering, 1024 Vagelos Research Laboratory, University of Pennsylvania, Philadelphia, Pennsylvania 19104, USA. E-mail: sld@seas.upenn.edu*

In order to test the efficiency of delivery of various siRNA transfection reagents and the pooled siRNA strategy, three siRNAs targeting Renilla luciferase were designed. Along with a scrambled negative control, the Renilla-targeting siRNAs were reverse transfected individually and pooled at total concentrations of 10 and 30 nmol/l under multiple conditions, followed by lipofection of Renilla pDNA and measurement of normalized luminescence (**Figure 1**). Reverse transfection of the pooled siRNAs with siPort NeoFX at a mass ratio of 1:3 resulted in silencing of the luminescence from Renilla pDNA by 88% as compared to the negative control. In addition, we optimized the Renilla pDNA dosage so as to arrive at delivery conditions that resulted in maximal Renilla luminescence signal with minimal toxicity (data not shown). This optimized dose was 0.02 µg Renilla luciferase pDNA/0.02 µl Lipofectamine 2000 per well of a 384-well plate.

Druggable genome HTS

Using the conditions arrived at as described, we carried out a HTS on the human druggable genome of siRNAs. The normalized transfection signal for each pool of siRNAs was calculated by dividing the luminescence from transfection by the luminescence from viability. The normalized transfection was further corrected for positional biases caused by edge effects, using an adapted median polish technique.[10–13] A robust *Z* score was calculated for each of the corrected data points to find siRNA pools causing significant improvements in normalized transfection (ref. 14 and **Figure 2**). Complete screening statistics for the primary screen are available in **Supplementary Table S1**. Pooled siRNA knockdowns that resulted in robust *Z* scores >2 on both replicate plates were identified as positive hits. Those that produced robust *Z* scores less than −2 on both replicate plates were identified as negative hits (inhibitors of lipofection). According to these criteria, 119 of the 5,520 gene targets qualified as positive hits, while 86 gene targets qualified as negative hits. Screening statistics for positive and negative hits are available in **Supplementary Tables S2** and **S3**, respectively. In order to supplement the list of positive hits, we selected an additional 11 gene targets that resulted in a significant increase in cell number following knockdown.

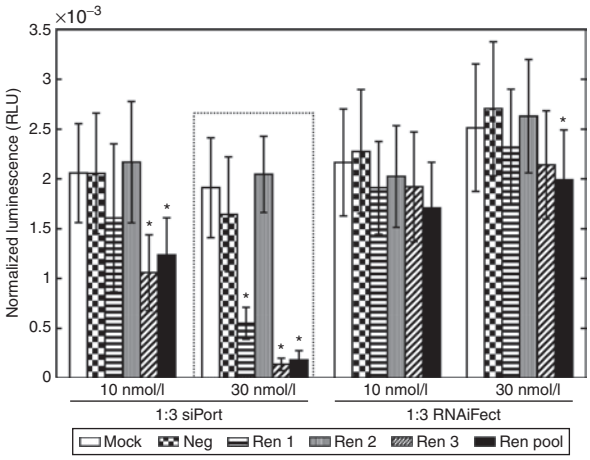

Figure 1 Human aortic endothelial cells were reverse transfected with sham control, negative control small-interfering RNA (siRNA), one of three siRNAs targeting the Renilla luciferase gene, or a pool of the three Renilla-targeting siRNAs. Two commercial transfection reagents, siPort NeoFX and RNAiFect, were used for reverse transfection. After siRNA reverse transfection and the subsequent lipofection of a Renilla luciferase plasmid DNA, luminescence from transfection and from viability were measured in each well, and from these data normalized luminescence was calculated. Each bar represents the mean-normalized luminescence, and the error bars represent 1 SD (n = 32). Significant changes with respect to the negative control (Neg) were determined using the Mann–Whitney *U*-test (*$P \leq 0.0001$). Ren, Renilla-targeted control; RLU, relative light unit; RNAi, RNA interference.

Confirmatory-screening assay

For each of the 130 gene targets corresponding to positive hits in the primary pooled screen, the three siRNAs were plated individually for confirmation. The individual siRNAs were reverse transfected into HAECs at 30 nmol/l using the same screening format as for the primary screen. The confirmatory screening assay was carried out in two independent experiments; the first screen was performed with all 130 primary screen positive hits (three siRNAs per gene) on three independent plates. From this round of screening, we identified 43 gene targets having at least one siRNA that produced an increase in luminescence from lipofection when compared with the negative control. These 43 genes (three siRNAs per gene) were rescreened on four independent plates at 30 nmol/l (a summary of the statistical data is included in **Supplementary Table S4**). The raw luminescence from lipofection for each point was compared against that of the negative control siRNA, and 18 of the genes were found to have at least two siRNAs that resulted in a significant change in transfection (**Table 1**). Of the 43 genes rescreened, 33 genes had at least one siRNA with a significant improvement in gene transfer. We selected 5 of the 33 confirmed gene targets as lead candidates to improve nonviral gene transfer: *PPP2R3A*, *PPP2R2C*, *GSK3β*,

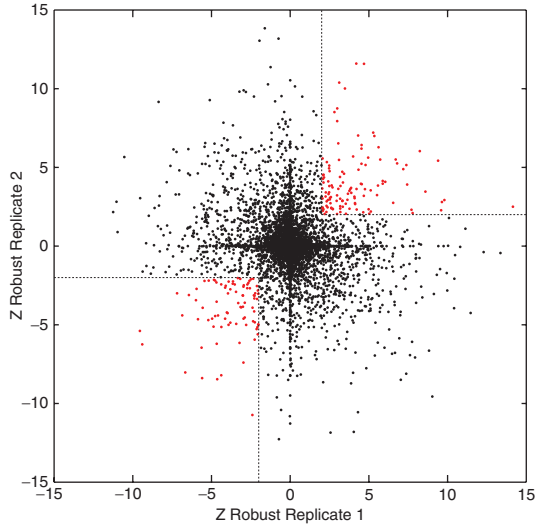

Figure 2 An RNA interference high-throughput screen was performed on 5,520 genes with three small-intefering RNAs pooled per gene in 384-well plates. Two replicates of each gene were screened in independent plates, and the robust *Z* score was calculated for each. Knockdowns resulting in a robust *Z* score of 2 or greater or −2 or less in both plates were identified as positive and negative hits, respectively, identified by the red dots in the figure.

Table 1 Confirmed gene targets

Gene	Gene symbol
Protease, serine, 23	*PRSS23*
Cytochrome P450, family 4, subfamily F, polypeptide 2	***CYP4F2***
Cathepsin B	***CTSB***
Protein kinase C–binding protein 1	*PRKCBP1*
Fibronectin leucine-rich transmembrane protein 1	***FLRT1***
Protein kinase, interferon-inducible double-stranded RNA dependent activator	*PRKRA*
Chloride channel 4	*CLCN4*
Aldehyde dehydrogenase 5 family, member A1	***ALDH5A1***
NAD(P)H: quinone oxidoreductase type 3, polypeptide A2	*NQO3A2*
ATPase, H+ transporting, lysosomal 56/58 kd, V1 subunit B, isoform 1	*ATP6V1B1*
Protein tyrosine phosphatase, nonreceptor type 3	*PTPN3*
Cytochrome P450, family 3, subfamily A, polypeptide 43	***CYP3A43***
Phospholipase C, delta 1	***PLCD1***
Solute carrier family 6 (neurotransmitter transporter, creatine), member 8	*SLC6A8*
Lecithin-cholesterol acyltransferase	***LCAT***
Transient receptor potential cation channel, subfamily M, member 2	*TRPM2*
ATP-binding cassette, subfamily A (ABC1), member 12	*ABCA12*
Euchromatic histone methyltransferase 1	*EHMT1*
T-cell activation GTPase activating protein	**TAGAP**
5,10-methenyltetrahydrofolate synthetase (5-formyltetrahydrofolate cyclo-ligase)	*MTHFS*
Protein phosphatase 2A, regulatory subunit B, α	***PPP2R3A***
Kallikrein B, plasma (Fletcher factor) 1	*KLKB1*
Killer cell lectin-like receptor subfamily B, member 1	*KLRB1*
A disintegrin-like and metalloprotease with thrombospondin type 1 motif, 8	*ADAMTS8*
Rho GTPase activating protein 4	***ARHGAP4***
FK506-binding protein 8, 38 kd	***FKBP8***
Protein phosphatase 2A, regulatory subunit B (PR 52), γ-isoform	***PPP2R2C***
MGC15668	***MGC15668***
Glycogen synthase kinase 3-β	***GSK3β***
Leucine-rich repeat-containing G protein–coupled receptor 6	***LGR6***
Interferon-γ receptor 2 (interferon-γ transducer 1)	***IFNGR2***
Protein tyrosine phosphatase, nonreceptor type 12	***PTPN12***
Ependymin related protein 1 (zebrafish)	***UCC1***

Abbreviation: ATP, adenosine triphosphate.
Gene targets with two or more confirmed small-interfering RNAs are shown in boldface font.

PRSS23, and *LCAT*. **Figure 3** displays the confirmatory screen results for the lead candidate gene targets in comparison with the scrambled negative control and the Renilla-targeting control. The Renilla-targeting control demonstrates that siRNA delivery in the confirmatory screen is effective, because the luminescence is silenced by 46% as compared to the scrambled negative

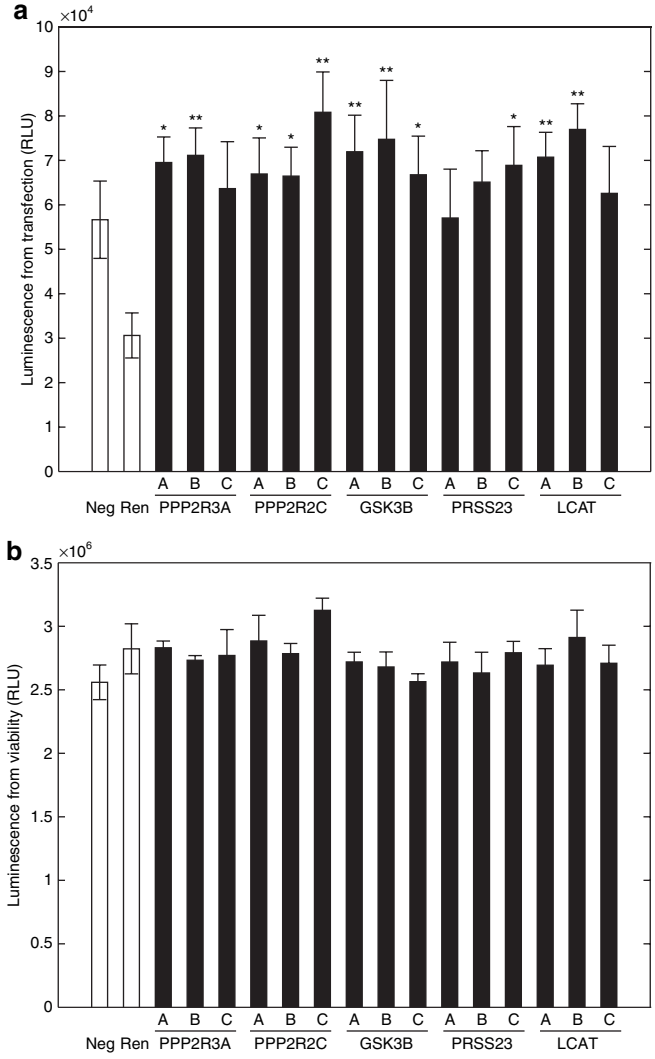

Figure 3 After the primary high-throughput screen, the three small-interfering RNAs (siRNAs) targeting the top positive hits were screened individually at 30 nmol/l. Luminescence data from (**a**) transfection and (**b**) viability are shown for the siRNAs corresponding to the five leading candidate genes, the negative control (Neg), and the Renilla-targeted control (Ren). Each bar represents the mean value, and error bars represent 1 SD ($n = 4$). Significant increases in transfection with respect to the negative control were calculated using the Mann–Whitney *U*-test (*$P \leq 0.05$ and **$P \leq 0.01$). RLU, relative light unit.

control. Gene silencing of each of the lead candidate gene targets produced enhancements in lipofection with at least one siRNA. Notably, in these confirmatory experiments, the number of cells determined by the luminescence from viability increased by 7–22% following *PPP2R3A* and *PPP2R2C* knockdown in all the siRNAs used.

Secondary screening assay

In order to test the effects of siRNA-mediated knockdown on the five lead gene targets in a larger-scale experiment, siRNAs were reverse transfected into HAECs in 96-well plates at 10 and 30 nmol/l. For each of the gene targets, we reverse transfected the three siRNAs targeting each gene in addition to the scrambled negative control. One day after siRNA reverse transfection, the cells were lipofected with

the Renilla luciferase pDNA and Lipofectamine 2000 using scaled conditions from the 384-well experiments. One day after pDNA lipofection, luminescence from Renilla luciferase (**Figure 4a**) and viability (**Figure 4b**) were measured for each well and averaged across the middle four wells for each condition.

The 96-well plate experiment was repeated on another day with replicates of four. The percentage of enhancement of normalized transfection relative to the negative control was calculated for each of the lead siRNAs, and the average from the two independent experiments was calculated. Six of the tested siRNAs resulted in enhanced nonviral transfection at the 96-well plate scale (**Table 2**).

GFP plasmid transfection and qRT-PCR

An investigation of the effectiveness of the six leading candidate siRNAs showed that silencing of the *PPP2R2C* and *PRSS23* genes demonstrated the largest potential for improving nonviral gene transfer. For validating the results of the luminescence assay, the siRNAs that were found to be most effective in targeting *PPP2R2C* and *PRSS23* were co-transfected with a green fluorescent protein (GFP) pDNA using Lipofectamine 2000. Fluorescence microscopy and flow cytometry analyses were performed one day after co-transfection (**Figure 5**). When an siRNA-targeting GFPwas co-delivered with GFP pDNA, the number of GFP-positive cells was reduced by about 27% relative to the nil-siRNA control. This finding demonstrates that the siRNA and pDNA were indeed effectively co-delivered. The number of cells successfully transfected with siRNA in the presence of *PPP2R2C* knockdown was 10% more than with the nil-siRNA control. By knocking down *PRSS23* using siRNA 19286, the number of transfected cells increased by 8%. Combining the knockdown of *PPP2R2C* and *PRSS23* by equal portions of siRNAs 104939 and 19286 caused an 8% increase in the number of transfected cells. In order to validate RNAi-mediated targeting of the *PPP2R2C* gene, HAECs were reverse transfected with siRNAs 104939, 104940, and 104941. Using quantitative real-time PCR (qRT-PCR), we confirmed that treatment with the three siRNAs against *PPP2R2C* resulted in ~76% gene silencing with siRNAs 104939 and 104940 and ~50% silencing with siRNA 104941 (**Figure 6**).

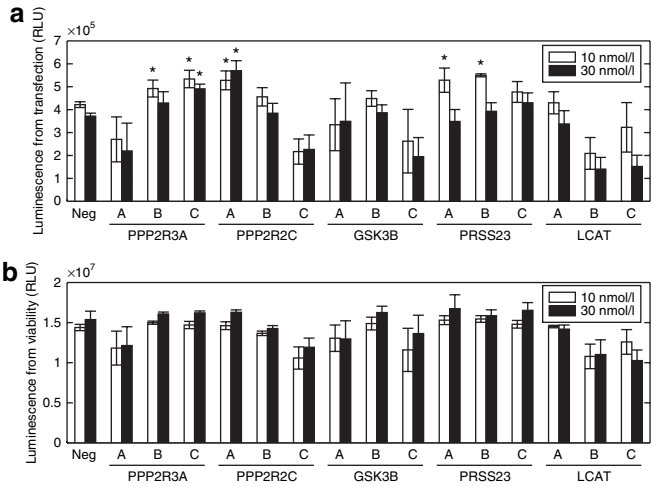

Figure 4 Lead candidates from the primary and confirmatory studies were screened in 96-well plates. (**a**) Raw transfection signal and (**b**) cell viability are shown after reverse transfection of small-interfering RNAs at 10 and 30 nmol/l with conditions scaled from the 384-well experiments. Each bar represents the mean value, and error bars represent 1 SD ($n = 4$). Significant increases in luminescence from lipofection with respect to the negative control were calculated using the Mann–Whitney *U*-test (*$P \leq 0.03$). Neg, negative control; RLU, relative light unit.

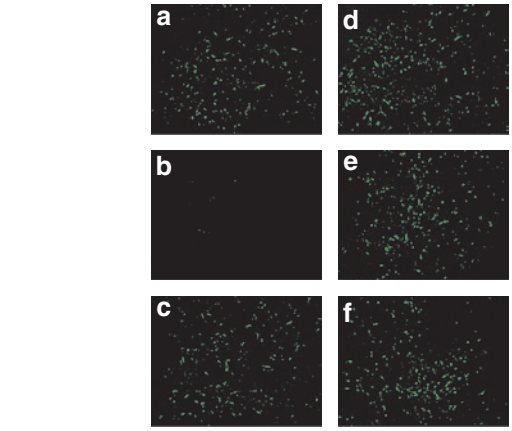

g

Region	Start bin	End bin	Lipo2000	No siRNA (a)	siGFP (b)	Neg (c)	104939 (d)	19286 (e)	104939 and 19286 (f)
R1	1	10	84.9	25.7	44.5	21.7	18.5	20.5	20.7
R2	10	50	2.6	13.1	21.6	13.3	13.5	13.7	13.1
R3	50	100	0.1	3.4	10.6	4.2	4.4	4.1	4.3
R4	100	500	0.1	9.2	11.9	10.9	11.6	12.1	12.3
R5	500	1,000	0.0	6.0	1.2	6.5	7.0	7.7	7.2
R6	1,000	5,000	0.0	21.4	1.6	23.2	26.6	24.9	25.0
R7	5,000	10,000	0.0	13.0	0.2	13.4	13.6	12.2	12.7
Total FL1 > 50			0.3	52.9	25.6	58.2	63.1	60.9	61.4
% Change from Lipo2000					−27.3	5.3	10.2	8.0	8.6

Figure 5 Human aortic endothelial cells were seeded 1 day prior to co-transfection with small-interfering RNAs (siRNAs) and green fluorescent protein (GFP) plasmid DNA using Lipofectamine 2000 (Lipo2000). The siRNAs co-delivered with plasmid were: (**a**) no siRNA; (**b**) GFP-targeting siRNA, siGFP; (**c**) negative control siRNA; (**d**) siRNA 104939; (**e**) siRNA 19286; and (**f**) siRNAs 104939 and 19286. Twenty-four hours after transfection, fluorescence microscopy pictures were taken (**a–f**). (**g**) The cells were subjected to flow cytometry analysis.

Table 2 Summary statistics for the lead candidate siRNAs

Gene symbol	siRNA label	siRNA ID	ASN sequence	% Change (10 nmol/l)	% Change (30 nmol/l)
PPP2R3A	B	104523	UCAAUGCUGGUAGGAUUCC	16	18
PPP2R3A	C	104525	UUAUGUCUUCAAGCAGGCC	39	23
PPP2R2C	A	104939	AGGUUGUAUCCUUCGGGCC	44	65
PPP2R2C	B	104940	GUGCAUGUCAGAGUUUACC	27	21
PRSS23	A	19286	AAUAAGAACAUGAAGACCC	48	10
PRSS23	B	19104	AGACAGAUAUUGCUUGGCC	33	16

Abbreviations: ASN, antisense; siRNA, small-interfering RNA.
Percent changes are calculated based on normalized transfection between sample and negative control, averaged over two independent experiments.

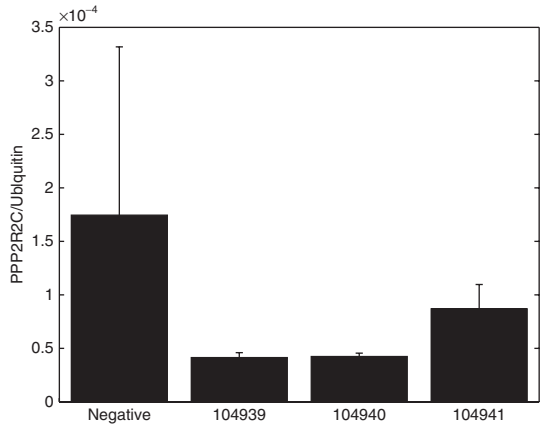

Figure 6 For quantitative real-time analysis, small-interfering RNAs (siRNAs) were reverse transfected into human aortic endothelial cells in 24-well plates, and RNA was harvested 24 hours later. The total RNA was reverse transcribed, and the PPP2R2C transcript was quantified for relative gene expression to verfiy the knockdown of the *PPP2R2C* gene. Each bar represents the mean value, and error bars represent 1 SD ($n = 4$ for all except for siRNA 104939, $n = 2$).

DISCUSSION

RNAi HTS can be used in diverse biological applications to understand the significance of gene pathways in parallel and to find proteins that are important to the process. RNAi libraries can target large portions of a human or mouse genome; the druggable genome siRNA library corresponds to gene targets that can ultimately be targeted with small-molecule therapies. For finding gene pathways that affect nonviral gene transfer, we developed an RNAi HTS strategy to screen the human druggable genome of siRNAs. We applied the HTS assay to confluent HAECs because nonviral vector transfection efficiencies are typically low, especially in comparison with those of viral vectors. As a model transfection reagent we used Lipofectamine 2000, a commercially available nonviral lipofection reagent, to deliver a reporter pDNA.

After delivery of pooled siRNAs and Renilla pDNA, gene knockdowns that enhanced nonviral gene transfer were identified as potentially rate-limiting (positive hits), and gene knockdowns that reduced nonviral gene transfer were identified as proteins potentially required for nonviral gene transfer (negative hits). After the primary screen of 5,520 druggable gene targets, ~2% of the gene targets were identified as positive hits while ~1.5% of the gene targets were identified as negative hit targets. The pooled siRNAs corresponding to the positive hit targets were subjected to confirmation and validation studies to find which of the individual siRNAs resulted in significant improvements in Lipofectamine 2000 gene transfer. After two rounds of confirmatory screening experiments, 33 genes were confirmed to enhance gene transfer upon silencing with one or more siRNAs, whereas 18 genes were confirmed to enhance gene transfer upon silencing with two or more siRNAs.

In order to confirm that these enhancements in gene transfer could be scaled to a larger format, we carried out the screening experiment in 96-well plates with the same Renilla luciferase pDNA and in 24-well plates with a GFP pDNA. We found that two siRNAs targeting the genes *PPP2R3A*, *PPP2R2C*, and *PRSS23* resulted in an average of 10–65% improvement in luminescence from transfection in 96-well plates. Two of these candidate gene targets, *PPP2R3A* and *PPP2R2C*, are different isoforms of the protein phosphatase 2A (PP2A) regulatory subunit. PP2A is known to mediate cell-cycle regulation through the M-phase-promoting factor, which regulates the G2/M transition.[15] The B regulatory subunit family of PP2A contains multiple subfamilies with multiple isoforms for each protein, each providing similar but unique regulation of PP2A activity. When siRNA 104939, targeting *PPP2R2C*, was co-transfected with GFP pDNA, flow cytometric analysis revealed an increase of 10% in the number of cells transfected, relative to the nil-siRNA control. Likewise, when an siRNA targeting an unrelated gene, *PRSS23*, was co-transfected with GFP pDNA, flow cytometric analysis revealed an 8% increase in the number of cells transfected. These findings show that the nearly twofold increases in luminescence in 96-well plates can be attributed to a greater number of cells being successfully transfected.

The finding that PPP2R2C targeting can enhance nonviral gene transfer is significant in the light of the known mechanisms of several viruses. Viral proteins such as human immunodeficiency virus-1 Viral Protein R, SV40 small t antigen, and others target subunits within the PP2A complex to aid in viral transduction.[9] Human immunodeficiency virus-1 Viral Protein R is known to interact with PP2A, and in fission yeast Viral Protein R was shown to interact specifically with the regulatory B subunits in a manner similar to the findings in this study, locking the cell population in G2/M, a susceptible state for infection.[16] SV40 targets the PP2A-A subunit and induces proliferation, which in turn enhances the transduction efficiency of the virus.[17] Both of these mechanisms take advantage of the natural mitotic breakdown of the nuclear envelope to shuttle the virus into the nucleus of the target cell. In this study, cell viability data show that silencing of the genes, *PPP2R3A* and *PPP2R2C* by multiple siRNAs results in cell number increases, thereby suggesting an increase in proliferation. These findings serve as preliminary evidence that the knockdown of *PPP2R3A* and *PPP2R2C* generates proliferation similar to that produced by several viruses. Despite these findings, further studies of cell-cycle mechanism are warranted in order to fully understand the role that RNAi gene silencing can play in cell-cycle regulation, and the potential applications to lipofection.

Previous work has identified the significance of the nuclear envelope as a transport barrier in gene transfer experiments.[18] For example, when a nonclassical nuclear-localization signal was used for assisting lipofection, the transfection was enhanced 100-fold in embryo-derived retinal ganglion cells.[19] Reports have also shown that even a high pDNA copy number (~10^4–10^5) surrounding the nucleus following a typical lipofection, is not a sufficient condition to produce a successful transfection event.[20] These previous reports suggest that the nuclear barrier is a significant barrier to successful transfection in confluent or nondividing cells, and that manipulation of the nuclear envelope would produce a successful transfection, such as during cell division. A report by Ludtke *et al.* suggested that the increase in transfection efficiency caused by cell division may be limited to twofold in certain cell types.[21] Our results are comparable to those of Ludtke *et al.*, with a 75% increase in raw luminescence (data not shown) and a 10% increase in the number of transfected cells after *PPP2R2C* knockdown. However, many genes contribute to cell-cycle regulation and there may be a locus of cell-cycle regulatory gene targets

that can ultimately lead to a larger enhancement in nonviral gene transfer, perhaps through similar siRNA or small-molecule inhibition. The limited enhancement observed here could also be a direct result of the use of Lipofectamine 2000 as the gene transfer reagent. Lipofectamine 2000 is known to be relatively efficient (albeit toxic), and other inefficient nonviral reagents may realize larger gains in transfection enhancement after *PPP2R2C* silencing.

The nuclear barrier is just one of many barriers that must be overcome, and appropriate mechanisms need to be incorporated into the vector design. For example, endosome escape is enhanced through the incorporation of neutral helper lipids in nonviral cationic-lipid gene transfer vectors.[22] Further research will reveal the best target to enhance gene transfer through cell cycle regulation; the siRNA(s) or small molecule inhibitor(s) targeting the requisite gene(s) or protein(s) could be paired with current nonviral delivery vectors to produce a delivery vehicle with pseudoviral vector properties.

In this study, we deployed siRNA screening to study nonviral gene transfer in HAECs. This technique can be easily adapted to other cell types and gene transfer techniques, and can point out the appropriate direction for researchers to follow in order to improve efficacy. In our system, we found that several cell-cycle-regulatory genes could be targeted for an enhancement in gene transfer; however screens with different systems may reveal different barriers worth targeting. This work demonstrates not only the utility of RNAi and its applications to nonviral gene transfer mechanisms, but also the potential for coupling siRNA and DNA in delivery vehicles for enhanced gene transfer efficiency.

MATERIALS AND METHODS

Cell culture. HAECs were maintained in culture at 37 °C and 5% CO_2 with EGM-2 endothelial media bullet kits (Cambrex Bio Science, Walkersville, MD). For transfections and RNA harvesting, cells were rinsed with Dulbecco's phosphate buffered saline and incubated with 0.05% Trypsin-EDTA (Gibco, Grand Island, NY).

Druggable genome library. The Silencer Human Druggable Genome library consisted of 5,520 gene targets, with three siRNAs per gene (Ambion, Austin, TX). The library was provided lyophilized at 0.25 nmol in 384-well plates, with the two right-hand columns left empty for controls. Each well was resuspended to a final concentration of 3,125 nmol/l and diluted to a concentration of 330 nmol/l using sterile nuclease-free water. The three wells with siRNAs corresponding to the same gene were combined in a pooled master in equal parts. The pooled master was then used to create assay plates containing pooled siRNAs. The final concentration of the pooled siRNAs in each assay well was 330 nmol/l in a volume of 2 µl. The well plates containing siRNAs were kept frozen at −80 °C until the screening day. For confirmatory screening experiments, individual siRNAs were cherry-picked from designated plates and plated at either 10 or 30 nmol/l, in the middle wells of a 384-well plate. For 96-well screening experiments, the siRNAs were ordered individually, resuspended in nuclease-free water, and preplated in a total volume of 4 µl.

High-throughput screening. For 384- and 96-well HTS experiments, cells were harvested and resuspended in full growth media so that the final seeding density would be 1.4×10^4 cells/cm^2. For reverse transfections, siRNAs were resuspended in a mixture of siPort NeoFX (Ambion) and Opti-MEM I Reduced Serum Medium (Gibco), allowing siRNA lipoplexes to form. Approximately 10 minutes later, cells in full growth media were added to the siRNAs so that the final screening concentration was either 10 or 30 nmol/l. The plates were covered with Breathe-Easy films (USA Scientific, Ocala, FL) and plastic lids, and placed in a cell culture incubator. One day later, the cells were lipofected with a cytomegalovirus-Renilla luciferase pDNA pGL4.75 (Promega, Madison, WI) with Lipofectamine 2000 (Invitrogen, Carlsbad, CA) in Opti-MEM I in accordance with the manufacturer's instructions (0.02 µg Renilla luciferase pDNA/0.02 µl Lipofectamine 2000 per well). After 20 minutes of incubation, 10 µl of the pDNA mixture was added to the assay plates, which were covered again with Breathe-Easy films and plastic lids, and placed in a cell culture incubator. One day after the pDNA lipofection, the cells were assessed for changes in luminescence. For measuring the luminescence from Renilla luciferase, EnduRen Live Cell Substrate (Promega) was mixed with full growth medium, and 10 µl was added to the each well at a final concentration of 20 µmol/l. The plates were allowed to incubate under cell culture conditions for 1.5 hours, and then tested for luminescence using an EnVision Multilabel Plate Reader (Perkin Elmer, Wellesley, MA). After analyzing for luminescence from lipofection, Cell-Titer Glo Luminescent Cell Viability Assay (Promega) was added in equal volume to each well. The plates were incubated at room temperature for ~30 minutes, and then subjected to a luminescence reading. The luminescent signal from Cell-Titer Glo is directly proportional to the adenosine triphosphate in each well, and is therefore a measure of the number of viable cells in the well.

HTS data analysis. After completing the HTS assay, the normalized transfection signal was calculated by dividing the luminescence from lipofection by the luminescence from viability. A median polish technique was used to correct for systematic row and column biases caused by edge evaporation.[11–13] The robust Z score was calculated for each point based on the interquartile range (IQR) and median (Med) of the set of screened data:

$$Z_{\text{robust}} = \frac{X_{\text{obs}} - \text{Med}}{\text{c} \cdot \text{IQR}}$$

where c is a constant of value 0.7413, so that the denominator is equivalent to 1 SD in a normal distribution, and X_{obs} is the normalized luminescence of the current observation.[14]

Large-scale siRNA reverse transfection. For qRT-PCR and flow cytometric analysis, siRNAs were reverse transfected in 24-well plates. The experimental siRNAs were mixed with siPort NeoFX in Opti-MEM I, in accordance with the manufacturer's instructions. Mixtures of 10 nmol/l siRNA and 1.3 µl siPort NeoFX per well were placed in the bottom of 24-well plates. The cells were trypsinized and resuspended, with 1.7×10^4 cells added to each well above the siRNA/siPort Neo FX mixture. Plates were covered with Breathe-Easy films and plastic lids, and placed in a cell culture incubator. One day later, RNA was collected or cells were lipofected with a GFP pDNA (pEGFP-N_3) (Clontech, Palo Alto, CA) using Lipofectamine 2000. pDNA and Lipofectamine 2000 were mixed with Opti-MEM I in accordance with the manufacturer's instructions (0.02 µg GFP pDNA/0.02 µl Lipofectamine 2000 per well). After 20 minutes of incubation, the pDNA mixture was added to the assay plates, which were covered again with Breathe-Easy films and plastic lids, and placed in a cell culture incubator.

Co-transfection of siRNAs and pDNA. Cells were preplated at 1.7×10^4 cells per well in 24-well plates one day prior to co-transfection. Lipoplexes of siRNAs and pDNA were created by mixing 0.43 µg siRNA(s) and 0.57 µg GFP pDNA with 1 µl Lipofectamine 2000 in Opti-MEM I. Complexes were added to cells as described, and harvested for flow cytometric analysis one day later.

Flow cytometry. One day after GFP pDNA lipofection, the cells were harvested for flow cytometry analysis and pooled to create a single, enriched sample. All flow cytometry data were collected without

compensation; the FL1 channel of the flow cytometer was used to collect and measure the GFP fluorescence. For measuring the percentage of cells transfected, FL1 signal intensities were gated in between the bins $10^0 < FL1 < 10^1$ (R1), $10^1 < FL1 < 5 \times 10^1$ (R2), $5 \times 10^1 < FL1 < 10^2$ (R3), $10^2 < FL1 < 5 \times 10^2$ (R4), $5 \times 10^2 < FL1 < 10^3$ (R5), $10^3 < FL1 < 5 \times 10^3$ (R6), and $5 \times 10^3 < FL1 < 10^4$ (R7).

Quantitative real-time PCR. After siRNA treatment, total RNA was isolated from each well using the Absolutely RNA microprep kit (Stratagene, La Jolla, CA). RNA was reverse transcribed using Superscript III reverse transcriptase and oligo(dT) (Invitrogen, Carlsbad, CA), and complementary DNA was purified using Qiagen's PCR purification kit (Valencia, CA). Complementary DNA from untreated samples was used for optimizing PCR conditions, with primers targeting the gene of interest. For the gene *PPP2R2C*, the forward primer was CATGTTCGATCGGAACACCAAGC and the reverse primer was CAGCTGTCCTCATCAGTGCTGTG.[23] In order to normalize the *PPP2R2C* gene, we used human *ubiquitin* as a housekeeping gene with forward primer GAGGTGGAGCCCAGTGACA and reverse primer ATGTTGTAGTCAGAAAGAGTGCGG. A standard curve was created using the untreated controls and the optimized PCR conditions for each set of primers on a Roche LightCycler (Indianapolis, IN). Quantitative real-time PCR was performed using the LightCycler FastStart DNA MasterPLUS SYBR Green I kit with melting curve analysis provided by the LightCycler software.

ACKNOWLEDGMENTS

We thank Sara Cherry (University of Pennsylvania, Philadelphia, PA) for assistance in RNAi HTS assay development and William Denney (Merck & Co., West Point, PA) for assistance and advice with data analysis and programming. This study was funded by the National Institutes of Health grant R01HL66565.

SUPPLEMENTARY MATERIAL

Table S1. Complete data for the primary high-throughput screen.
Table S2. Complete data for the positive hits of the primary high-throughput screen.
Table S3. Complete data for the negative hits of the primary high-throughput screen.
Table S4. Summary of the confirmatory screening results.

REFERENCES

1. Ruponen, M, Honkakoski, P, Ronkko, S, Pelkonen, J, Tammi, M and Urtti, A (2003). Extracellular and intracellular barriers in non-viral gene delivery. *J Control Release* **93**: 213–217.
2. Lechardeur, D and Lukacs, GL (2002). Intracellular barriers to non-viral gene transfer. *Curr Gene Ther* **2**: 183–194.
3. Lechardeur, D, Verkman, AS and Lukacs, GL (2005). Intracellular routing of plasmid DNA during non-viral gene transfer. *Adv Drug Deliv Rev* **57**: 755–767.
4. Mukherji, M, Bell, R, Supekova, L, Wang, Y, Orth, AP, Batalov, S *et al.* (2006). Genome-wide functional analysis of human cell-cycle regulators. *Proc Natl Acad Sci USA* **103**: 14819–14824.
5. Rines, DR, Gomez-Ferreria, MA, Zhou, Y, DeJesus, P, Grob, S, Batalov, S *et al.* (2008). Whole genome functional analysis identifies novel components required for mitotic spindle integrity in human cells. *Genome Biol* **9**: R44.
6. Berns, K, Hijmans, EM, Mullenders, J, Brummelkamp, TR, Velds, A, Heimerikx, M *et al.* (2004). A large-scale RNAi screen in human cells identifies new components of the p53 pathway. *Nature* **428**: 431–437.
7. Willingham, AT, Deveraux, QL, Hampton, GM and Aza-Blanc, P (2004). RNAi and HTS: exploring cancer by systematic loss-of-function. *Oncogene* **23**: 8392–8400.
8. Brass, AL, Dykxhoorn, DM, Benita, Y, Yan, N, Engelman, A, Xavier, RJ *et al.* (2008). Identification of host proteins required for HIV infection through a functional genomic screen. *Science* **319**: 921–926.
9. Zhao, RY and Elder, RT (2005). Viral infections and cell cycle G2/M regulation. *Cell Res* **15**: 143–149.
10. Malo, N, Hanley, JA, Cerquozzi, S, Pelletier, J and Nadon, R (2006). Statistical practice in high-throughput screening data analysis. *Nat Biotechnol* **24**: 167–175.
11. Velleman, PF and Hoaglin, DC (1981). *Applications, Basics, and Computing of Exploratory Data Analysis*. Duxbury: Boston, MA. pp. 354.
12. Hoaglin, DC, Mosteller, F and Tukey, JW (2000). *Understanding Robust and Exploratory Data Analysis*. Wiley: New York. pp. 447.
13. Hoaglin, DC, Mosteller, F and Tukey, JW (2006). *Exploring Data Tables, Trends, and Shapes*. Wiley-Interscience: Hoboken, NJ. pp. 527.
14. Zhang, XD, Yang, XC, Chung, N, Gates, A, Stec, E, Kunapuli, P *et al.* (2006). Robust statistical methods for hit selection in RNA interference high-throughput screening experiments. *Pharmacogenomics* **7**: 299–309.
15. Janssens, V and Goris, J (2001). Protein phosphatase 2A: a highly regulated family of serine/threonine phosphatases implicated in cell growth and signalling. *Biochem J* **353**: 417–439.
16. Elder, RT, Yu, M, Chen, M, Zhu, X, Yanagida, M and Zhao, Y (2001). HIV-1 Vpr induces cell cycle G2 arrest in fission yeast (*Schizosaccharomyces pombe*) through a pathway involving regulatory and catalytic subunits of PP2A and acting on both Wee1 and Cdc25. *Virology* **287**: 359–370.
17. Rundell, K and Parakati, R (2001). The role of the SV40 ST antigen in cell growth promotion and transformation. *Semin Cancer Biol* **11**: 5–13.
18. Lechardeur, D and Lukacs, GL (2006). Nucleocytoplasmic transport of plasmid DNA: a perilous journey from the cytoplasm to the nucleus. *Hum Gene Ther* **17**: 882–889.
19. Ma, H, Zhu, J, Maronski, M, Kotzbauer, PT, Lee, VM, Dichter, MA *et al.* (2002). Non-classical nuclear localization signal peptides for high efficiency lipofection of primary neurons and neuronal cell lines. *Neuroscience* **112**: 1–5.
20. Tseng, WC, Haselton, FR and Giorgio, TD (1997). Transfection by cationic liposomes using simultaneous single cell measurements of plasmid delivery and transgene expression. *J Biol Chem* **272**: 25641–25647.
21. Ludtke, JJ, Sebestyen, MG and Wolff, JA (2002). The effect of cell division on the cellular dynamics of microinjected DNA and dextran. *Mol Ther* **5**: 579–588.
22. Wasungu, L and Hoekstra, D (2006). Cationic lipids, lipoplexes and intracellular delivery of genes. *J Control Release* **116**: 255–264.
23. Hu, P, Yu, L, Zhang, M, Zheng, L, Zhao, Y, Fu, Q *et al.* (2000). Molecular cloning and mapping of the brain-abundant B1gamma subunit of protein phosphatase 2A, PPP2R2C, to human chromosome 4p16. *Genomics* **67**: 83–86.